Optical Predistortion Enabling Phase Preservation in Optical Signal Processing Demonstrated in FWM-based Amplitude Limiter

K. R. H. Bottrill, F. Parmigiani, D. J. Richardson, P. Petropoulos

***Abstract*—We propose and demonstrate a technique to obtain phase preservation in optical processing which is suitable for many four-wave mixing (FWM) based processing devices, provided they may be modified to incorporate two conjugating FWM stages. It functions by using a first conjugating nonlinear stage to predistort the signal using self-phase modulation (SPM) such that when the signal undergoes further SPM in a second conjugating FWM stage, the two SPM contributions negate each other, resulting in phase preserving output. In this work, we use the second stage to perform amplitude squeezing through parametric gain saturation and characterise the scheme by regenerating a QPSK signal contaminated with broadband amplitude noise. Experimental analysis of the system with and without predistortion is provided and phase preserving operation using the proposed scheme is confirmed.**

I. Introduction

Processing a signal using four wave mixing (FWM) is typically associated with a concomitant exposure of the signal to self-phase modulation (SPM). Excessive exposure to SPM is typically avoided by reducing the power with which a signal is launched into a nonlinear processing device, however this approach comes at the expense of reduced optical signal to noise ratio (OSNR). This trade-off between OSNR and SPM distortion is generally present whenever FWM processes are used, whether it is for wavelength conversion [1], [2], phase quantisation [3], [4] or amplitude limitation [5], [6], and ultimately limits the performance that can be obtained from such nonlinear processing devices.

It has been shown in the context of a saturated, pump-degenerate FWM-based amplitude limiter, that amplitude to phase noise conversion can be suppressed by pursuing the use of a pump power much greater than the signal power [7], and although it is only in the limit of infinite pump to signal power ratio that amplitude noise to phase noise conversion due to the signal's own amplitude variation is completely suppressed, useful levels of suppression can be realised for modest increases in pump to signal power ratio. In order to allow saturation to be achieved using a lower signal power (and hence higher pump to signal power ratio), it is necessary to increase one or more of the following factors: pump power (P_0), nonlinear coefficient (γ) or medium length (L) [7]. This approach is not only applicable to amplitude limiters, but also in general to any other process involving FWM between a pump (or pumps) and a signal.

However, whilst such an approach is, in itself, simple to adopt, it is not necessarily easy to implement. Practical issues typically constrain the extent to which the three factors, P_0, γ and L can be increased, such as power limitations set to avoid damage, nonlinear coefficients constrained by the available technology and medium lengths set to avoid excessive loss or inconvenient size. Aside from these issues, however, which mainly present themselves as engineering problems, nonlinear media typically also present a further nonlinear phenomenon, stimulated Brillouin scattering (SBS), which is well known to limit the maximum power of narrow linewidth pumps which can be launched into the medium. However, the ramifications of SBS go beyond simply setting limits on launch power, and this can be illustrated mathematically by considering the definition for the nonlinear coefficient (in which n_2 is the nonlinear refractive index, ω_0 is the carrier frequency of the light and c is the speed of light) [8]:

$$\gamma = \frac{n_2 \omega_0}{c A_{eff}} \tag{1}$$

and a formulation for the Brillouin threshold [9]:

$$P_{th} = \frac{21 b A_{eff}}{g_B L} \tag{2}$$

where b is a polarisation factor representing the relative polarisation of the pump and Stokes waves with range $1 \leq b \leq 2$ (1 in the case that linear polarisation is maintained, 2 if polarisation is scrambled [10]), and g_B is a gain factor specific to the medium in question. For simplicity, let us assume that our goal is to maximise the nonlinear phase shift given by $\Phi = P_0 \gamma L$. We set the pump power, P_0, below the Brillouin threshold given by Equation 2, as in general we may not practically go beyond this value. Now, if we expand the nonlinear coefficient using Equations 1 and 2, we obtain the following nonlinear phase shift:

$$\Phi \leq \frac{21 b A_{eff}}{g_B L} \frac{n_2 \omega_0}{c A_{eff}} L = \frac{21 b n_2 \omega_0}{g_B c} \tag{3}$$

which shows us that the maximum nonlinear phase shift obtainable without inciting SBS can neither be increased by lengthening the medium nor by decreasing the effective area to more tightly confine the light. Hence, other means of increasing the maximum net nonlinear shift must be sought, such

This research is sponsored by EPSRC grant EP/I01196X, The Photonics Hyperhighway. Dr F. Parmigiani is supported by a Royal Academy of Engineering/EPSRC research fellowship.

The data for this work is accessible through the University of Southampton Institutional Research Repository (DOI:10.5258/SOTON/399384).

The authors are affiliated with the Optoelectronics Research Centre, University of Southampton, SO17 1BJ, UK.

as increasing n_2, altering g_B or attenuating the backscattered light. This issue explains the popularity of methods such as pump phase dithering [11], straining of the highly nonlinear fibre (HNLF) [12] or the use of optical isolators between HNLF spans [13] to mitigate SBS.

To overcome the discussed challenges we propose in this paper the following: instead of trying to avoid amplitude to phase noise conversion, we accept its occurrence and adopt an approach of mitigation. In essence, the signal is first predistorted with SPM during an initial conjugating nonlinear stage, before it undergoes a second conjugating stage during which the optical processing is performed and any SPM accrued here in the second stage acts to undo the SPM of the first stage. Although the first and second stage may perform a variety of processing tasks, in the present case the first stage is used simply to perform the predistortion, whilst the second performs amplitude regeneration through saturated pump degenerate FWM; in another demonstration [14], the first stage was used to perfom phase regeneration whilst the second compensated for phase to amplitude noise conversion using an amplitude limiter, with SPM negation between the two stages effectively resulting in a system which was greater than the sum of its two parts. The advantages of the proposed approach are that it permits relatively high signal powers to be used without compromising the signal quality due to SPM, resulting in higher achievable output OSNRs whilst relaxing the requirements placed on the system, such as the need for high pump power or extensive SBS mitigation. An additional feature of this approach is that its mechanism of action is one of *compensation* rather than simply *reduction*, this means that SPM induced distortions can be eliminated completely with more modest efforts than those needed when pursuing a high pump to signal power ratio. In addition, as the operating principle of the scheme makes use of two conjugating stages, the system is naturally capable of undoing pump phase dither, and so we may take advantage of this effect to increase the maximum pump launch powers permissible before the onset of SBS, in order to obtain even better OSNRs.

II. Operating Principle

Figure 1-a illustrates a scenario where an amplitude noise loaded QPSK signal is subject to SPM as it undergoes amplitude squeezing through gain saturation in FWM. SPM can be seen to transform the radial distribution of the constellation plots such that they follow the familiar anticlockwise spiral associated with SPM. The combination of SPM and amplitude squeezing can be seen to result in a signal which, although having a reduced amplitude noise, has experienced an increase in phase noise. The severity of these effects has been shown [7] to depend only upon the pump to signal power ratio used to achieve saturation, with phase preserving operation being achieved in the limit of large pump to signal power ratio (when the pump is assumed noiseless, see [15], [16] for a discussion of the impact of noisy pumps). Achieving a large enough pump to signal power ratio to sufficiently prevent amplitude noise to phase noise conversion may, however, present something of a practical challenge. Indeed, to demonstrate this approach in [7], a total launch power of $34\,\mathrm{dBm}$ and a concatenation of several HNLFs with a total length of $1.5\,\mathrm{km}$ was used, with optical isolators between several spans. The proposed method is somewhat less challenging to implement, and we shall discuss it next.

In the following description of the proposed scheme, we shall make use of the theoretical results presented in [7], which were obtained by making use of an exact solution to FWM in the dispersionless case [11], [17], [18]. Figure 2 outlines the procedure followed in the scheme. In the first step (illustrated by Figure 2 -1), a pump, P_0 is multiplexed with the signal P_1 and then allowed to undergo FWM in a medium of length L_1 and nonlinear coefficient γ_1 in the second step (Figure 2 -2), after which the conjugate of the signal is selected using an optical bandpass filter. The output power and phase of this conjugate can be shown [7], [11], [18] to be given by Equations 4 and 5, respectively, where J_n is the nth Bessel function of the first kind, and J_n^2 its square. In [7] we identified two sources of amplitude to phase noise conversion which can be seen to originate from the following phase shift terms in Equation 5: SPM, given by $\Delta\phi_{SPM} = \gamma_1 L_1 P_1$ and Bessel Order Mixing (BOM), given by $\Delta\phi_{BOM} = \arctan\left\{\frac{\sqrt{P_0}J_{-1}(2\sqrt{P_0P_1}\gamma_1 L_1)}{\sqrt{P_1}J_{-2}(2\sqrt{P_0P_1}\gamma_1 L_1)}\right\}$ (which can also be seen to depend upon pump power). For the present discussion, their origin is not important, although their dependence upon the signal power, P_1, reveals their nature as a cause of amplitude noise to phase noise conversion.

Given the means of operation of the scheme, it is important that during this first, predistortion stage, the amplitude of the signal is *not* squeezed. SPM effectively instigates a one to one amplitude to phase shift mapping; the phase is shifted by an amount which depends on its power. This mapping must be preserved if it is to be easily undone in the following stage, as the amplitude of the signal indicates the phase shift it has experienced in the previous stage.

The second stage is implemented, in essence, identically to the first, but receives the filtered conjugate of the original signal (Figure 2-3) as input and so undoes the wavelength conversion and conjugation of the first stage, although this time the powers of the pump and signal are chosen to ellicit saturation of the gain of the conjugate, squeezing its amplitude [7]. This process is illustrated by stages 4 and 5 of Figure 2 before and after FWM. Conjugation during this stage effectively reverses the phase shift experienced by the signal during the first stage. This is illustrated in Figure 1-b, where it can be seen that, after the first stage, the symbol clusters follow an anticlockwise spiral, whereas during FWM in the second stage, they follow a clockwise spiral. SPM in this second stage can now be seen to undo the SPM of the first stage, and so the system results in a decrease in amplitude noise with no further increase in phase noise. This stage, similarly to the first, can be described by Equations 6 and 7 where Q_n and θ_n represent the powers and phases of the various harmonics for the second system, i.e. the following variable changes have occured $P_n \rightarrow Q_n$ and $\phi_n \rightarrow \theta_n$.

The signal input to the second stage is the conjugate output of the first stage. Figure 3 provides plots of the conjugate

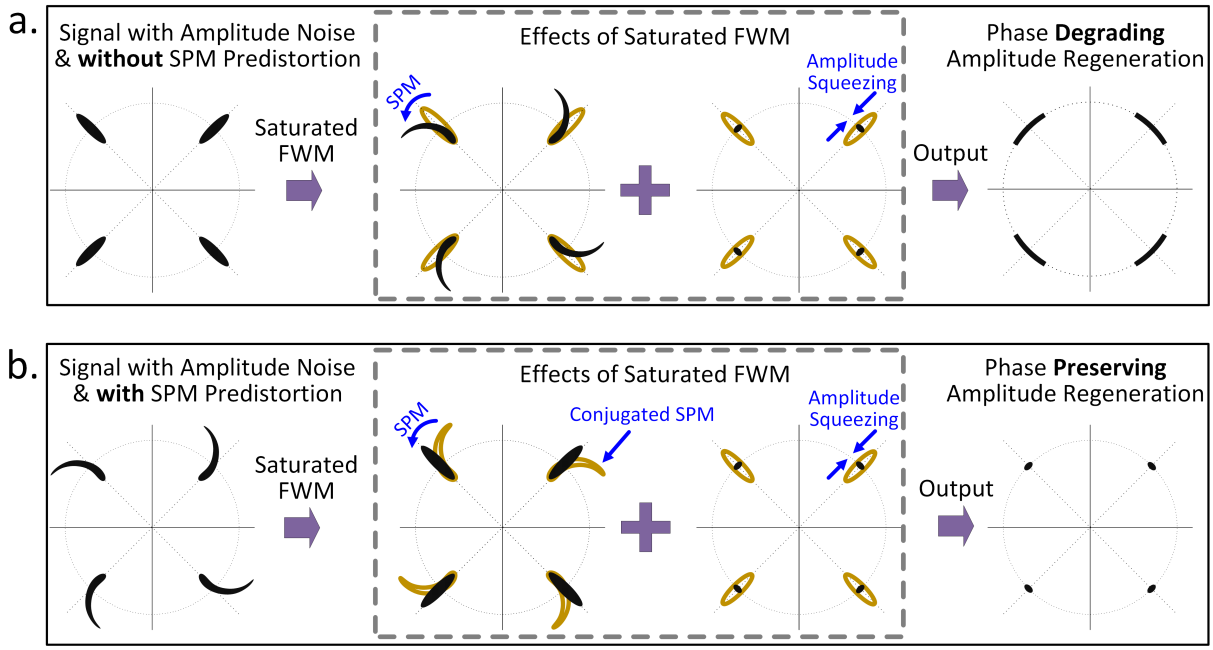

Fig. 1. Illustrations of saturated FWM-based amplitude limiter: a) *without* optical SPM predistortion b) *with* optical SPM predistortion.

$$P'_{-1} = P_0 J^2_{-1}(2\sqrt{P_0 P_1}\gamma_1 L_1) + P_1 J^2_{-2}(2\sqrt{P_0 P_1}\gamma_1 L_1) \tag{4}$$

$$\phi'_{-1} = 2\phi_0 - \phi_1 + \gamma_1 L_1 P_0 + \gamma_1 L_1 P_1 + \arctan\left\{\frac{\sqrt{P_0}J_{-1}(2\sqrt{P_0 P_1}\gamma_1 L_1)}{\sqrt{P_1}J_{-2}(2\sqrt{P_0 P_1}\gamma_1 L_1)}\right\} \tag{5}$$

$$Q'_{-1} = Q_0 J^2_{-1}(2\sqrt{Q_0 Q_1}\gamma_2 L_2) + Q_1 J^2_{-2}(2\sqrt{Q_0 Q_1}\gamma_2 L_2) \tag{6}$$

$$\theta'_{-1} = 2\theta_0 - \theta_1 + \gamma_2 L_2 Q_0 + \gamma_2 L_2 Q_1 + \arctan\left\{\frac{\sqrt{Q_0}J_{-1}(2\sqrt{Q_0 Q_1}\gamma_2 L_2)}{\sqrt{Q_1}J_{-2}(2\sqrt{Q_0 Q_1}\gamma_2 L_2)}\right\} \tag{7}$$

$$\begin{aligned}\theta'_{-1} = {} & \phi_1 + 2\theta_0 - 2\phi_0 + \gamma_2 L_2 Q_0 + \gamma_2 L_2 Q_1 - \gamma_1 L_1 P_0 - \gamma_1 L_1 P_1 \\ & + \arctan\left\{\frac{\sqrt{Q_0}J_{-1}(2\sqrt{Q_0 Q_1}\gamma_2 L_2)}{\sqrt{P_{-1}}J_{-2}(2\sqrt{Q_0 Q_1}\gamma_2 L_2)}\right\} - \arctan\left\{\frac{\sqrt{P_0}J_{-1}(2\sqrt{P_0 P_1}\gamma_1 L_1)}{\sqrt{P_1}J_{-2}(2\sqrt{P_0 P_1}\gamma_1 L_1)}\right\}\end{aligned} \tag{8}$$

$$\begin{aligned}\theta'_{-1} = {} & \phi_1 + \gamma_2 L_2 Q_1 - \gamma_1 L_1 P_1 \\ & + \arctan\left\{\frac{\sqrt{Q_0}J_{-1}(2\sqrt{Q_0 Q_1}\gamma_2 L_2)}{\sqrt{P_{-1}}J_{-2}(2\sqrt{Q_0 Q_1}\gamma_2 L_2)}\right\} - \arctan\left\{\frac{\sqrt{P_0}J_{-1}(2\sqrt{P_0 P_1}\gamma_1 L_1)}{\sqrt{P_1}J_{-2}(2\sqrt{P_0 P_1}\gamma_1 L_1)}\right\}\end{aligned} \tag{9}$$

output power (Q'_{-1}, given by Equation 6) as it varies with signal input power (Q_1) for three different operating scenarios defined by their pump power, Q_0 =24 dBm, Q_0 =31 dBm and Q_0 =36 dBm, plotted for $\gamma_2 L_2 = 1$. It can be seen that each curve possesses a value of Q_1 which results in a peak in output power, hence, to achieve saturation, Q_1 must be operated about this value, which can be achieved by attenuating or amplifying the output of the first stage, P'_{-1}, as required. It is interesting to note that, for the Q_0 =31 dBm case, the peak in conjugate output power is noticeably broadened as compared to the other cases and so may result in improved amplitude squeezing. This is due to the coefficients of $J_1(x)$ and $J_2(x)$ in Equation 6 being of comparable magnitude.

As we have a means of controlling Q_1 to achieve saturation, we have no further interest in expanding the expression for Q_1. We are, however, interested in expanding θ'_{-1}, so that we can understand the output phase of the signal after it has passed through both stages. Substituting $\theta_1 = \phi'_{-1}$ into Equation 7 and expanding using Equation 5 leads to Equation 8 after simplification. Provided that the linewidth of the pumps is sufficiently narrow and their RIN is sufficiently low, $2\phi_0$, $2\theta_0$, $\gamma_1 L_1 P_0$ and $\gamma_2 L_2 Q_0$ all constitute constant phase shifts and so can be neglected. Setting these values to zero, Equation 8 can be reduced to Equation 9.

From here, it is relatively clear that SPM can be completely negated between the two stages by tuning Q_1 such that

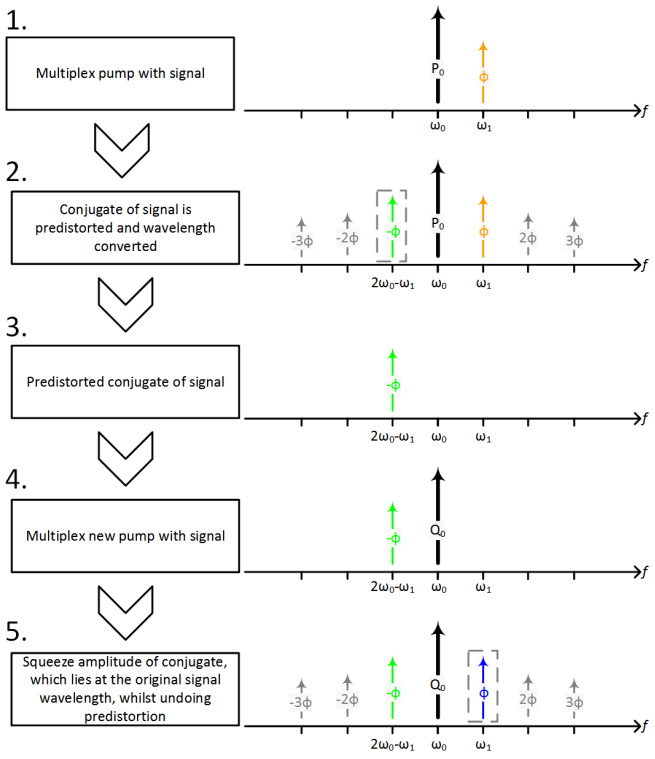

Fig. 2. Stages of the phase preserving amplitude regenerator.

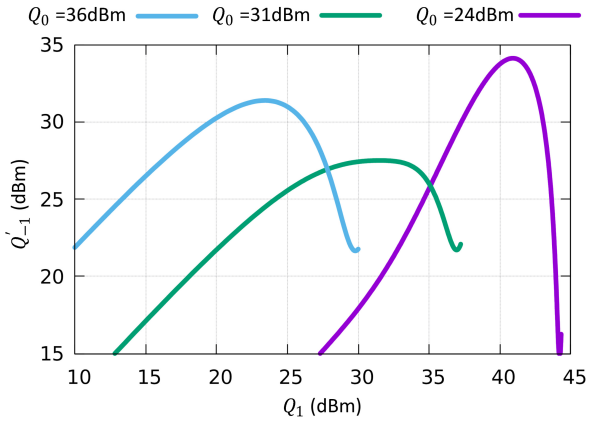

Fig. 3. Conjugate output power as it varies with signal input power for three different pump levels.

$\gamma_2 L_2 Q_1 = \gamma_1 L_1 P_1$. Negating the effects of BOM, on the other hand is not so straightforward. Although uncompensated BOM is of less consequence than SPM [7], it does nonetheless represent a source of amplitude to phase noise conversion. Fortunately, the SPM predistortion of the first stage can be used to compensate for the BOM of the second stage to some degree as well. To demonstrate the efficacy of this approach to BOM suppression, we shall consider a model case where the amplitude limiting second stage is operated with $[Q_0 : Q_1]_{Sat} = -0.5\,\mathrm{dB}$, which results in the most severe BOM. Hence, our conclusions should represent a worse case scenario for this approach, of offsetting BOM in the second stage using the SPM of the first stage.

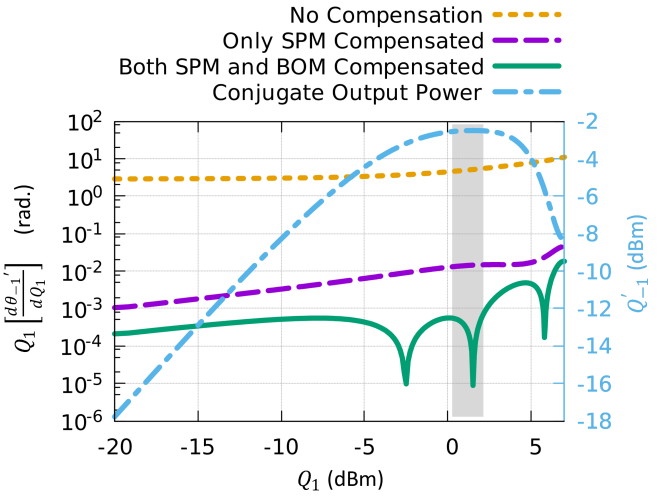

Fig. 4. Operating the amplitude saturator with $[Q_0 : Q_1]_{Sat} = -0.5\,\mathrm{dB}$ - Left axis: Phase derivatives for 3 cases: without predistortion (yellow short dashed line); with only SPM compensation (purple long dashed line); with both SPM and BOM compensation (green solid line). Right axis shows conjugate output power, plotted with blue dash-dot line with grey band showing region of operation for amplitude squeezing.

As discussed in [7], it is the derivative of phase with power which determines the amplitude to phase noise conversion of the FWM process. Figure 4 provides, on the left axis, plots of these derivatives for three scenarios, along with a plot of the output power of the conjugate on the right axis, with the operating region highlighted by a grey band. The first derivative plotted corresponds to the case when no SPM predistortion is used (yellow, short dashed line), and so represents the case of using a single, conjugating amplitude saturator operating with $[Q_0 : Q_1]_{Sat} = -0.5\,\mathrm{dB}$. If SPM predistortion is used only to compensate for the SPM of the second, amplitude saturating stage, the phase derivative obtained is that shown by the purple line with long dashes. The severity of amplitude to phase noise conversion in the region of operation can be seen to decrease by two to three orders of magnitude, with this plot effectively describing the residual phase noise due to BOM. If we now attempt to compensate for both the SPM *and* BOM of the final stage, using SPM predistortion, we obtain the solid green curve. The phase derivative can be seen to be decreased by at least a further factor of 10. Hence, SPM predistortion shows a very impressive ability to reduce BOM. As we have considered the pump to signal ratio which ellicits maximum BOM, we should expect the system to operate even better away from this pump to signal power ratio.

III. Experimental Setup

The experimental set-up used is shown in Figure 5, with the various stages color-coded for clarity. The pumps (P_0 and Q_0) were sourced from the same, 192.6 THz laser, which was phase-dithered using a 93 MHz sine wave to increase the SBS threshold in the two HNLFs. To undo the effects of the pump phase dithering, the phase dither on the pump in the second stage must be correctly synchronised with the residual phase dither present on the output of the first stage. Given the fixed path length difference between the two pumps and the signals

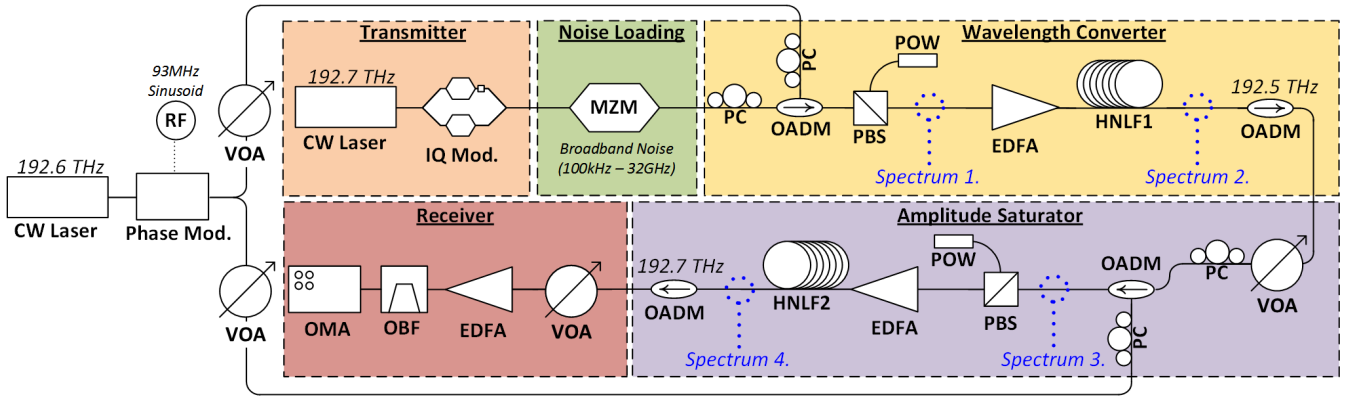

MZM=Mach-Zehnder Modulator, PC=Polarization Controller, PBS=Polarization Beam Splitter, POW=Power Meter, AWG=Arrayed Waveguide Grating, HNLF=Highly Nonlinear Fiber, OMA=Optical Modulation Analyzer, OBF=Optical Bandpass Filter, RF=Radio Frequency Signal, OADM=Optical Add-Drop multiplexer

Fig. 5. Experimental set-up.

with which they mix, tuning the frequency of the phase dither can be seen to shift the relative phase of the dither on each pump. Hence, dither negation was achieved by fine tuning of the dither frequency.

A second laser, operating at 192.7 THz, was launched into an IQ modulator to generate a 10 GBaud QPSK signal. The modulated signal then entered a noise-loading stage wherein it was contaminated with broadband amplitude noise by modulating it with a Mach-Zehnder modulator driven by ASE that had been detected using a photodiode and amplified electrically. It was then fed to the first, wavelength converting stage, where it was multiplexed with P_0 using an optical add-drop multiplexer (see corresponding spectrum in Figure 6-1). Before multiplexing, the pump and signal passed through polarisation controllers which were used to ensure they were copolarised by minimising the off-axis power measured from a polarisation beam splitter which lay in their common path. The pump and signal were then amplified using an EDFA before being launched into HNLF1, which consisted of 1km of unstrained low dispersion HNLF, formed by connecting to HNLF spools directly to each other in series. Given the low dispersion of the HNLFs as well as the small frequency separation between the pump and signal, dispersion is of little consequence to the system, predominantly representing a small reduction in FWM efficiency and a modification to the exact pump and signal powers required to achieve saturation. A pump to signal power ratio, $P_0 : P_1$, of 1.5 dB was used at the input of HNLF1, with a total power of 20.5 dBm, tuned to provide the appropriate amount of SPM predistortion, determined using an optimisation process which will be discussed later. The wavelength converted phase conjugate (see Figure 6-2) was selected using an optical add-drop multiplexer (OADM) after which it entered the second nonlinear stage.

In the second nonlinear stage, similarly to the first, the conjugate output of the first stage was multiplexed with pump Q_0, (resulting in the spectrum given in Figure 6-3) before passing through a polarisation beam splitter to allow their polarisations to be aligned. They were then amplified using an EDFA before being launched into HNLF2. As before, HNLF2 was comprised of multiple fibre segments totalling

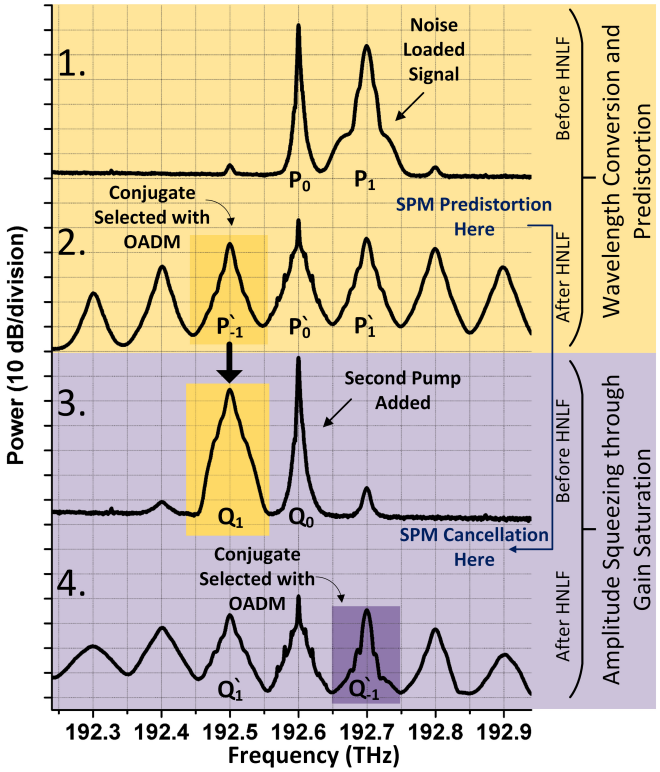

Fig. 6. Experimentally measured spectral traces: 1. before SPM predistortion; 2. after SPM predistortion; 3. before amplitude squeezing; 4. after amplitude squeezing. Numerical labels correspond to locations indicated in Figure 5.

580 m in length, but this time the fibres were strained to increase the Brillouin threshold. The total power launched into HNLF2 was 25 dBm and the pump to signal power ratio, $Q_0 : Q_1$, was 6 dB. The output of this stage lay at the original wavelength of 192.7 THz (see Figure 6-4), was amplitude limited, unconjugated relative to the original, and, of course, had benefitted from the SPM predistortion of the first stage. The signal was selected using an OADM and analysed using an optical modulation analyser (OMA).

As discussed, the scheme functions by balancing the amplitude to phase noise distortion induced by both the first

and second stages. Practical issues aside, for any choice of Q_1, there should always be a corresponding value of P_1 which minimises amplitude noise to phase noise conversion. We exploit this flexibility to prioritise other factors in the system, namely, the maximisation of output OSNR without resorting to further means of SBS suppression. Maximising output OSNR leads us to choose a pump power in the second stage, Q_0, just below the brillouin threshold of the fibre, and a relatively high signal power of about $19\,\mathrm{dBm}$, which necessarily results in the signal being exposed to substantial SPM. It is important to remember that we would not be able to the increase signal power to such a large extent if the technique of optical predistortion had not been adopted, as the signal would be exposed to an intolerable amount of SPM. With the launch powers of the second stage selected, the required pump and signal launch powers of the first stage could be found. To obtain a first estimate for the signal power required to be launched into the first stage, P_1, we ignore BOM and assume amplitude to phase noise conversion arises only due to SPM. We then set the requirement:

$$P_1\gamma_1 L_1 = Q_1\gamma_2 L_2 \Rightarrow P_1 = \frac{Q_1\gamma_2 L_2}{\gamma_1 L_1} \tag{10}$$

Substituting the known parameters into the right hand side of Equation 10 (where we use the effective length of the relevant fibres for L_1 and L_2) leads to an estimate of the required power with which the signal is to be launched into the first stage of $P_1 \approx 20.5\,\mathrm{dBm}$. To fine tune this estimate, a blind optimisation algorithm was used which trialled successive values of P_1, searching for a value which minimised $\Delta\phi_{out}$, the output phase noise of the signal at the receiver, after regeneration. This process led to an optimal value for P_1 of $19\,\mathrm{dBm}$ being found, which we believe is in reasonable agreement with the analytical estimate above, given the approximation used in the calculation (neglect of BOM) and the accuracy of the measurements made. During the optimisation process, the signal was loaded with amplitude noise so a measureable output phase noise ($\Delta\phi_{out}$) could be detected for optimisation and minimised, and care was taken to ensure that the first stage was operated outside of the saturation regime.

To demonstrate the benefit of adopting the dual stage approach, the system was also operated as a single stage regenerator by bypassing the first, wavelength converting stage in Figure 5 and squeezing the signal using the same total launch power into the amplitude limiter. The results of these two means of operation were compared with the signal before regeneration.

IV. Experimental Results

Figure 7 shows constellation diagrams of the signal before regeneration (top row), after single-stage regeneration (middle row) and after dual-stage regeneration (bottom row), for 6 different input amplitude noise scenarios. These amplitude noise scenarios were achieved by loading the signal with amplitude noise prior to regeneration using the noise loading stage shown in Figure 5, and are quantified by their root mean squared amplitude variation, ΔMag_{in}. The constellation plots for an input amplitude noise of $\Delta Mag_{in} = 8.1\,\mathrm{deg.\ rms}$ correspond to the case when no noise was added to the signal, and show a small improvement in amplitude noise after regeneration with either the single stage or dual stage scheme due to the non-ideal amplitude noise of the transmitter. Both regenerators also result in a small increase in phase noise, possibly due to incomplete dither compensation, residual amplitude noise to phase noise conversion or OSNR degradation.

As input amplitude noise is increased, both regenerators can be seen to reduce amplitude noise to approximately the same level. However, drastic differences can be seen between their phase noise behaviour. For the single stage regenerator, increasing the amplitude noise can be seen to result in a strong increase in the phase noise of its output. In contrast, the dual stage regenerator seems to exhibit no such increase, with phase noise appearing reasonably constant until an input amplitude noise of $\Delta Mag_{in} = 16.8\%\ \mathrm{rms}$, after which both the amplitude noise and phase preservation can be seen to be slightly compromised. For $\Delta Mag_{in} = 24.2\%\ \mathrm{rms}$, which can be seen to correspond to substantial amplitude noise in the unregenerated case, we are no longer able to decode the signal output of the single stage regenerator due to the extent of phase noise, however, for the dual stage scheme the signal can be detected quite well and still shows a great improvement in signal quality over the unregenerated signal.

Figure 8 provides plots of the output magnitude noise, ΔMag_{out}, (Figure 8-a) and output phase noise, $\Delta\phi_{out}$, (Figure 8-b) as they vary with ΔMag_{in} for three scenarios: before regeneration (open orange circles), after regeneration with the single stage regenerator (green struck circles) and after regeneration with the dual stage regenerator (blue, crossed circles). Data was obtained using the same OMA as the constellation diagrams, but is given for ΔMag_{in} over a larger range of $8\%\ \mathrm{rms}$ to $42\%\ \mathrm{rms}$. Considering first Figure 8-a, both the single stage and dual stage schemes can be seen to offer very similar performance in terms of amplitude regeneration, with both resulting in a large reduction in magnitude noise, although the single-stage regenerator falls behind the dual-stage regenerator for $\Delta Mag_{in} > 15\%\ \mathrm{rms}$, a reason for which will be offered in the next paragraph. The greatest reduction in magnitude noise for the dual-stage regenerator can be seen for $\Delta Mag_{in} = 18.9\%\ \mathrm{rms}$, for which an output magnitude noise of $\Delta Mag_{out} = 6.4\%\ \mathrm{rms}$ is obtained, which is only $1/3$ of the input noise. The output noise of both regenerators increases with increasing input noise, which is to be expected, as amplitude squeezing is performed by an instantaneous peak in the power transfer function, and is not truly constant with input power. For the most extreme case tested, the dual-stage regenerator still manages to reduce amplitude noise from $\Delta Mag_{in} = 41.9\%\ \mathrm{rms}$ to $\Delta Mag_{in} = 23.2\%\ \mathrm{rms}$, a reduction of almost $1/2$.

Turning our attention now to the output phase noise plots shown in Figure 8-b, the superiority of the dual-stage approach can be clearly seen. The dual-stage regenerator results in a small, but effectively constant increase in output phase noise, $\Delta\phi_{out}$, of about $1\,\mathrm{deg.\ rms}$, all the way up to the most severe test case. This indicates the absence of amplitude to phase noise conversion, and so we conclude that the small deterioration that does occur is predominantly caused by

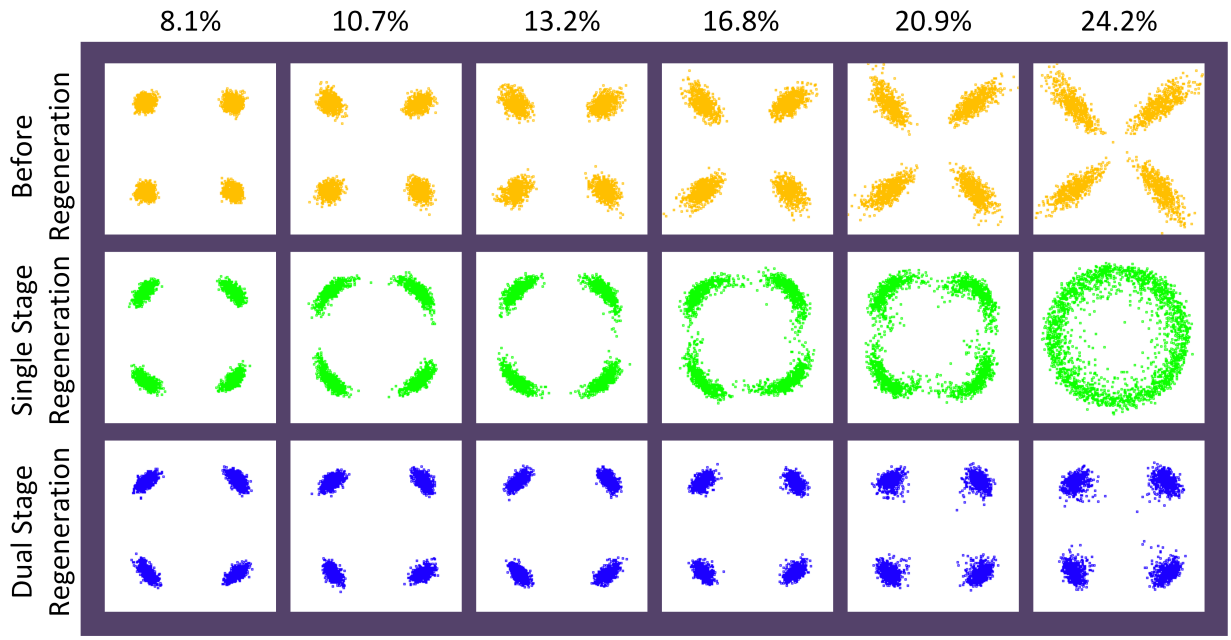

Fig. 7. Experimentally measured constellation diagrams: before regeneration (top row), after regeneration with single stage regenerator (middle row) and after regeneration with single stage regenerator (bottom row) for 6 different input amplitude noise levels.

OSNR degradation during the FWM processes and imperfect dither cancellation. In stark contrast, for the single-stage regenerator, $\Delta\phi_{out}$ increases linearly with increasing input magnitude noise, up until $\Delta Mag_{in} \approx 20\%$ rms, after which point the recorded data is omitted, as the severity of the phase degradation prevented the OMA from successfully performing phase tracking. Indeed, the impact of the phase noise upon phase tracking is responsible for the increased spread of the single-stage regenerator measurements over their unregenerated and dual-stage counterparts as well as being a potential cause of the apparently reduced performance of the single-stage regenerator as compared the dual-stage regenerator for higher input magnitude noises in Figure 8-a.

Finally, BER curves are presented in Figure 9 for the unregenerated signal (plotted in orange) and for the signal regenerated using the dual stage scheme (plotted in blue) along with linear fits. Results for the single stage case were not collected as, based upon the noise statistics and constellation diagrams shown previously, they would only be worse than those obtained using the dual stage regenerator. ΔMag_{in} was controlled, as before, using the amplitude noise loading stage which sits just after the transmitter and before the wavelength converting stage. The OSNR at the receiver, which is plotted on the x-axis of Figure 9, was controlled by attenuating the signal after it had been regenerated but before it was launched into the receiver EDFA indicated in Figure 5 and BERs were measured using the OMA (intradyne detection with an independent local oscillator). For the case when no additional noise was added to the signal, the regenerator can be seen to result in approximately no power penalty. For a high input noise case of $\Delta Mag_{in} = 18.3\%$ rms (see Figure 7 for reference), the dual stage regenerator can be seen to result in an improvement in receiver sensitivity at all BERs recorded, and specifically for a BER of 10^{-5}, a 3.3 dB improvement compared to the unregenerated case is shown.

V. Conclusions

We have proposed and experimentally demonstrated a phase preserving FWM-based amplitude limiter using two simple pump degenerate FWM stages. The first stage is used to perform optical phase predistortion such that nonlinear phase rotation accrued in a subsequent stage is grossly reduced. It was shown theoretically that SPM, the most important cause of amplitude noise to phase noise conversion, may be completely mitigated using this technique whilst BOM, a lesser but nonetheless important source of amplitude noise to phase noise conversion can be reduced by a considerable margin. An almost threefold reduction of the amlitude magnitude noise is demonstrated on a QPSK signal for an initial magnitude error of $\Delta Mag_{in} = 14.5\%$ rms, while the corresponding output phase noise remains quite constant with increasing input amplitude noise. The dual stage regenerator was compared to a single stage approach implemented by bypassing the predistortion stage, but using the same total launch power to achieve saturation. The dual stage regenerator shows a near constant output phase noise, whereas the single stage regenerator shows a seemingly linear increase in output phase noise with increasing input amplitude noise on the signal, highlighting the advantages of the demonstrated scheme. Importantly, this scheme is not only applicable to the case of amplitude regeneration demonstrated here, indeed, in general any FWM based signal processing scheme which incorporates, or may be extended to incorporate two FWM stages, may exploit the technique to increase output OSNRs without compromising the signal quality due to amplitude noise to phase noise conversion, provided the amplitude to

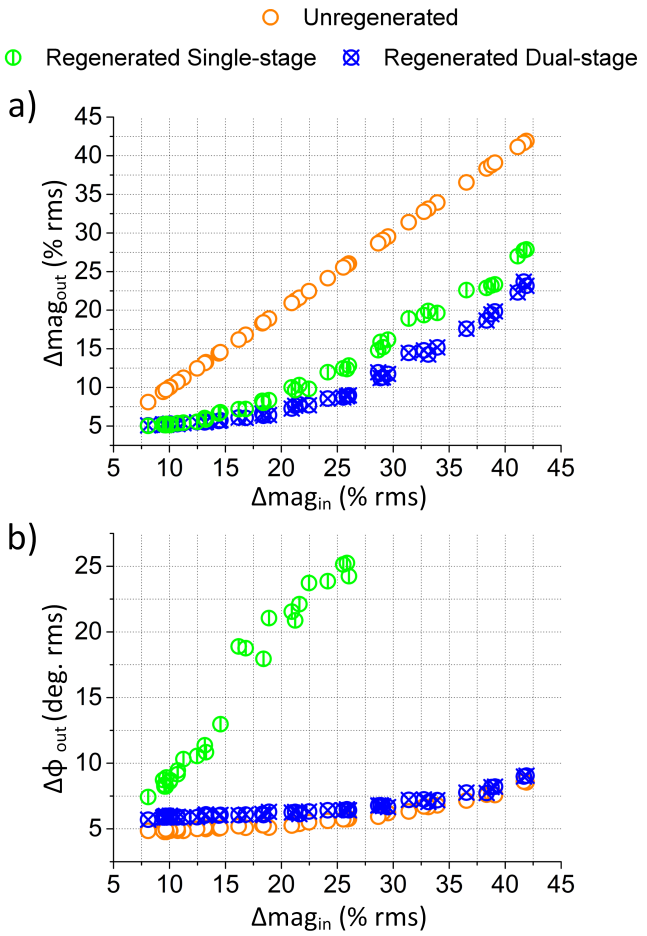

Fig. 8. Noise statistics as they vary with input magnitude noise for three scenarios, the unregenerated case, single-stage regeneration and dual-stage regeneration. a) Output magnitude noise; b) Output phase noise.

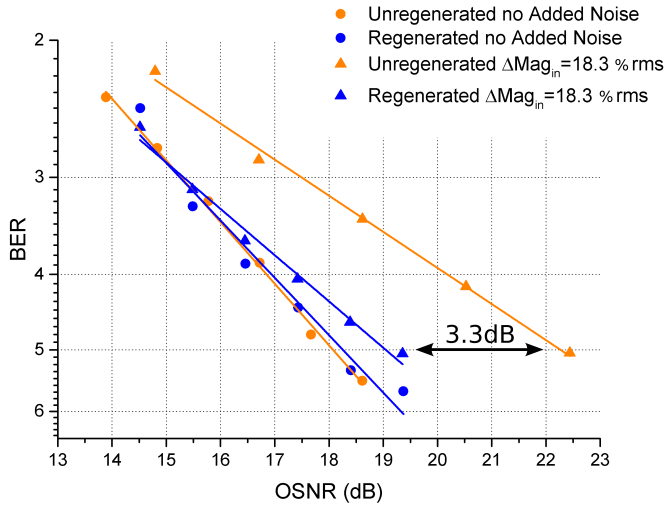

Fig. 9. BERs with (blue symbols) and without (orange symbols) regeneration for two noise scenarios, without additional magnitude noise (circles) and with $\Delta Mag_{in} = 18.3\%$ rms.

phase mapping is preserved until the final stage. The attractiveness of this approach can be increased further if the two nonlinear processing stages are performed in two counter-propagating modes of the same fibre. Additionally, the first, predistorting, nonlinear stage used in this scheme can be employed to perform constructive signal processing of its own, as was shown, for instance, in [14] where the first stage was used to perform phase regeneration, whilst the second was used to perform amplitude squeezing.

References

[1] S. Yoo, "Wavelength conversion technologies for wdm network applications," *Lightwave Technology, Journal of*, vol. 14, no. 6, pp. 955–966, Jun 1996.

[2] T. Inoue, K. Tanizawa, and S. Namiki, "Guard-band-less and polarization-insensitive tunable wavelength converter for phase-modulated signals: Demonstration and signal quality analyses," *J. Lightwave Technol.*, vol. 32, no. 10, pp. 1981–1990, May 2014.

[3] J. Kakande, R. Slavk, F. Parmigiani, A. Bogris, D. Syvridis, L. Grner-Nielsen, R. Phelan, P. Petropoulos, and D. J. Richardson, "Multilevel quantization of optical phase in a novel coherent parametric mixer architecture," *Nature Photonics*, vol. 5, no. 12, pp. 748–752, Dec. 2011.

[4] S. L. I. Olsson, B. Corcoran, C. Lundström, T. A. Eriksson, M. Karlsson, and P. A. Andrekson, "Phase-sensitive amplified transmission links for improved sensitivity and nonlinearity tolerance," *J. Lightwave Technol.*, vol. 33, no. 3, pp. 710–721, Feb 2015.

[5] Z. Lali-Dastjerdi, M. Galili, H. C. H. Mulvad, H. Hu, L. K. Oxenløwe, K. Rottwitt, and C. Peucheret, "Parametric amplification and phase preserving amplitude regeneration of a 640 gbit/s rz-dpsk signal," *Opt. Express*, vol. 21, no. 22, pp. 25 944–25 953, Nov 2013.

[6] M. Matsumoto and T. Kamio, "Nonlinear phase noise reduction of dqpsk signals by a phase-preserving amplitude limiter using four-wave mixing in fiber," *Selected Topics in Quantum Electronics, IEEE Journal of*, vol. 14, no. 3, pp. 610–615, May 2008.

[7] K. R. H. Bottrill, G. Hesketh, F. Parmigiani, D. J. Richardson, and P. Petropoulos, "Optimisation of amplitude limiters for phase preservation based on the exact solution to degenerate four-wave mixing," *Opt. Express*, vol. 24, no. 3, pp. 2774–2787, Feb 2016.

[8] G. P. Agrawal, *Nonlinear fiber optics*. Amsterdam [u.a.: Elsevier/Acad. Press, 2007.

[9] R. G. S. P. Singh and N. Singh, "Nonlinear scattering effects in optical fibers," *Progress in Electromagnetics Research*, vol. 74, pp. 379–405, 2007.

[10] R. H. Stolen, "Polarization effects in fiber raman and brillouin lasers," *Quantum Electronics, IEEE Journal of*, vol. 15, no. 10, pp. 1157–1160, Oct 1979.

[11] M. E. Marhic, *Fiber optical parametric amplifiers, oscillators and related devices*. Cambridge: Cambridge University Press, 2012.

[12] N. Yoshizawa and T. Imai, "Stimulated brillouin scattering suppression by means of applying strain distribution to fiber with cabling," *Journal of Lightwave Technology*, vol. 11, no. 10, pp. 1518–1522, 1993.

[13] Y. Takushima and T. Okoshi, "Suppression of stimulated brillouin scattering using optical isolators," *Electronics Letters*, vol. 28, no. 12, pp. 1155–1157, Jun. 1992.

[14] K. R. H. Bottrill, F. Parmigiani, L. Jones, G. Hesketh, D. J. Richardson, and P. Petropoulos, "Phase and amplitude regeneration through sequential psa and fwm saturation in hnlf," in *Optical Communication (ECOC), 2015 European Conference on*, Sept 2015, pp. 1–3.

[15] M. Matsumoto, "Phase noise generation in an amplitude limiter using saturation of a fiber-optic parametric amplifier," *Opt. Lett.*, vol. 33, no. 15, pp. 1638–1640, Aug 2008.

[16] G. Hesketh, K. R. H. Bottrill, F. Parmigiani, D. J. Richardson, and P. Petropoulos, "On the role of signal-pump ratio in fwm-based phase preserving amplitude regeneration," in *International Conference on Optical Networks ICTON '15*, July 2015.

[17] C. J. McKinstrie and M. G. Raymer, "Four-wave-mixing cascades near the zero-dispersion frequency," *Opt. Express*, vol. 14, no. 21, pp. 9600–9610, Oct 2006.

[18] E. Lichtman, A. A. Friesem, R. G. Waarts, and H. H. Yaffe, "Exact solution of four-wave mixing of copropagating light beams in a kerr medium," *J. Opt. Soc. Am. B*, vol. 4, no. 11, pp. 1801–1805, Nov 1987.